ARTICLE IN PRESS

BMB Reports - Manuscript Submission

Manuscript Draft

Manuscript Number: BMB-18-245

Title: Elimination of Double-Strand Break End Resection Switches Recombination to the Non-homologous End Joining Pathway During Meiosis in Saccharomyces cerevisiae

Article Type: Article

Keywords: double-strand breaks; non-homologous end-joining; homologous recombination; Ku complex; meiosis

Corresponding Author: Keunpil Kim

Authors: Keunpil Kim[1,*], Hyeseon Yun[1]

Institution: [1]Life Science, Chung-Ang University,

UNCORRECTED PROOF

ARTICLE IN PRESS

BMB *Reports*

Elimination of Double-Strand Break End Resection Switches Recombination to the Non-homologous End Joining Pathway During Meiosis in *Saccharomyces cerevisiae*

Hyeseon Yun[1] and Keunpil Kim[1,*]

[1]Department of Life Science, Chung-Ang University, Seoul 06974, Korea

[*]**Corresponding Author:**
Keunpil Kim
Department of Life Sciences
Chung-Ang University
Seoul 156-756
Korea
E-mail: kpkim@cau.ac.kr
Phone: 82-2-820-5792
Fax: 82-2-820-5206

Running title: Activation of non-homologous end joining in meiosis

UNCORRECTED PROOF

ARTICLE IN PRESS

ABSTRACT

During meiosis, programmed double-strand breaks (DSBs) are repaired via recombination pathways that are required for faithful chromosomal segregation and genetic diversity. In meiotic progression, the non-homologous end joining (NHEJ) pathway is suppressed and instead meiotic recombination initiated by nucleolytic resection of DSB ends is the major pathway employed. This requires diverse recombinase proteins and regulatory factors involved in the formation of crossovers (COs) and non-crossovers (NCOs). In mitosis, spontaneous DSBs occurring at the G1 phase are predominantly repaired via NHEJ, mediating the joining of DNA ends. The Ku complex binds to these DSB ends, inhibiting additional DSB resection and mediating end joining with Dnl4, Lif1, and Nej1, which join the Ku complex and DSB ends. Here, we report the role of the Ku complex in DSB repair using a physical analysis of recombination in *Saccharomyces cerevisiae* during meiosis. We found that the Ku complex is not essential for meiotic progression, DSB formation, joint molecule formation, or CO/NCO formation during normal meiosis. Surprisingly, in the absence of the Ku complex and functional Mre11-Rad50-Xrs2 complex, a large portion of meiotic DSBs was repaired via the recombination pathway to form COs and NCOs. Our data suggested that impaired DSB resection channels meiotic recombination through the NHEJ pathway, which is also required for the maintenance of genomic integrity.

Keywords: double-strand breaks, non-homologous end-joining, homologous recombination, Ku complex, meiosis

UNCORRECTED PROOF

ARTICLE IN PRESS

INTRODUCTION

DNA double-strand breaks (DSBs) are the most toxic form of DNA lesions generated by various types of DNA damaging agents, such as free radicals, ultraviolet light, and ionizing radiation (1-4). To repair DSBs, cells induce tightly regulated DNA repair programs such as homologous recombination and non-homologous end joining (NHEJ) that are highly conserved in all eukaryotic organisms. The choice of repair program between NHEJ and recombination depends on cell cycle phase and the process of DSB ends (5-7). For homologous recombination to proceed to repair spontaneous DNA damage and meiotic Spo11-catalyzed DSBs, many recombinase proteins and chromosome structural proteins play an important role. Homologous recombination utilizes the sister chromatid (or homologs in diploids) as a template for the repair of accidental DSBs during mitosis (8-11). Unlike mitosis, however, meiotic DSBs are repaired via the recombination pathway to achieve genetic diversity for the next generation. In meiotic recombination, DSB ends predominantly utilize the homologous chromosome as a template for homology search and strand exchange to produce non-identical gametes by exchanging genetic information (12).

Meiotic recombination is initiated by programmed DSBs induced by the meiosis-specific topoisomerase II-like protein Spo11 (13). For recombination to progress, the highly conserved Mre11-Rad50-Xrs2 (MRX in yeast; Mre11-Rad50-Nbs2 in mammals) complex binds to DSB regions and controls end resection to remove Spo11 (14-16). DSB end resection during S and G2 phases of the cell cycle is achieved through cyclin-dependent kinase (CDK)-mediated phosphorylation of Sae2, an essential factor for activating the DNA endonuclease of the MRX complex, which is associated with bridging DNA ends (17-19). Exonucleases, such as Exo1 and Dna2-Sgs1, resect the 5′-ends of DNA strands to generate 3′ single-strand DNA (ssDNA) that is required for recombinase binding and homology searching (20). Replication protein A (RPA)—a heterotrimeric complex consisting of Rfa1, Rfa2, and Rfa3—binds to the ssDNA of

UNCORRECTED PROOF

DSB ends to inhibit secondary structures formed by ssDNA self-complementizing or to protect DSB ends from degradation (21). After displacement of RPA from ssDNA, Rad51, a RecA homolog, forms nucleofilaments that are also used for homology searching and homolog pairing during mitosis. However, in meiotic recombination, Rad51 functions as an auxiliary factor of Dmc1 for homolog bias (9).

NHEJ, a prominent DSB repair pathway of the mitotic cell cycle, mediates direct re-ligation of DSB ends from spontaneous DNA damage. NHEJ is initiated by a DNA end binding complex, the Ku70-Ku80 heterodimeric complex (Ku complex), which prevents 5′ strand resections of DSB ends (17, 22). Once the Ku complex binds to the DSB ends, it serves as a core site of NHEJ accessory factor recruitment to the DNA breaks. Inaccurate end-joining as a result of Ku complex-deficiency causes chromosomal breaks and aneuploidy (23). In budding yeast, DNA end processing involved in the NHEJ pathway is mediated by diverse factors including Dnl4 (ATP-dependent ligase; DNA ligase IV in vertebrates), Lif1 (XRCC4 in vertebrates), Nej1 (XLF in vertebrates), and Pol4 (Pol μ and Pol λ in vertebrates) (24-27). The DNA end bridge complex is targeted by a DNA ligase complex that mediates end-joining of DSB ends and inhibits DSB end resection, which is processed by nuclease-helicase enzymes (24-27). Finally, Pol4 and Lig4 are required for filling in the DNA gaps (25). In mammalian cells, DSB repair via homologous recombination utilizes the sister chromatid as a template because it is nearby during the S/G2 phase, while NHEJ is the major DSB repair process that occurs in all cell cycle phases. The Ku complex binds to a DNA end to form the Ku:DNA complex that serves as a platform where a ligase complex including XLF, XRCC4, and DNA ligase IV can dock to rejoin the ends (25-27). However, it is not well understood whether the NHEJ pathway is involved in meiosis or whether the Ku complex is required for the repair of meiotic DSBs.

Here, we investigated the role of the NHEJ pathway and the relationship between the Ku

UNCORRECTED PROOF

ARTICLE IN PRESS

and MRX complexes. Experimental studies of NHEJ-mediated meiotic DSB repair are challenging because recombination is the major DSB repair pathway in meiosis. To this end, we examined meiotic recombination in *Saccharomyces cerevisiae* through physical analysis of recombination.

RESULTS

The Ku complex is not essential for meiotic division and spore viability

The Ku complex rapidly localizes to DSB sites and is involved in protecting DNA ends from nuclease-helicase processing as well as recruiting NHEJ proteins (25). To provide insights into the role of the Ku complex during meiosis, we observed meiotic division and spore formation in wild-type (WT) and *ku70Δ* mutant cells (Fig. 1A and 1B). Meiosis was induced in cells incubated in sporulation medium (SPM) that were then harvested from the culture at different time points (0, 2.5, 3.5, 4, 5, 6, 7, 8, 10, and 24 h). In WT cells, meiotic division began after 5 h in sporulation media and rapidly progressed with 50% of cells having underwent division after approximately 6 h. In *ku70Δ* cells, normal nuclear division occurred with a slight delay of about 20 min compared with that of WT (Fig. 1A). Moreover, DAPI staining indicated that both WT and *ku70Δ* cells exhibited normal nuclei separation after 24 h; 91.4% and 4.2% of *ku70Δ* cells produced four and three spores, respectively, compared with the 92% and 3% of WT, respectively (Fig. 1B and 1C). Thus, *ku70Δ* cells underwent meiosis normally and formed viable spores as did the WT, confirming that NHEJ is not an essential pathway for repairing Spo11-induced DSBs. To understand the role of the Ku complex in mitotic DNA damage repair, we employed the methyl methane sulfonate (MMS) sensitivity test in the absence of the Ku complex (Fig. 1C and 1D). *ku70Δ* cells grew at similar levels as the WT in YPD media containing 0.01% and 0.03% MMS (Fig. 1D). Thus, DNA damage of vegetative cells is not

UNCORRECTED PROOF

ARTICLE IN PRESS

lethal for *ku70Δ* mutants, indicating that NHEJ is not an essential pathway in MMS-induced DSB repair.

Physical analysis of meiotic recombination

To determine the molecular pathway involved in meiotic recombination, we monitored recombination intermediates and final outcomes (crossovers [COs] and non-crossovers [NCOs]) using the *HIS4LEU2* assay system for chromosome III (Fig. 2). In the *HIS4LEU2* assay system, COs and NCOs can be detected after digesting genomic DNA with XhoI and NgoMIV enzymes. After synchronizing yeast cells at the G1 phase in pre-sporulation medium (SPS), the cells were transferred to sporulation medium to initiate meiosis. Cells were then treated with psoralen after harvesting to produce interstrand-crosslink DNA, which stabilizes single-end invasions (SEIs) and double-Holliday junctions (dHJs; 8-10, 28, 29). Meiotic DNA samples were digested with XhoI and then DNA fragments were analyzed by DNA gel electrophoresis and Southern blotting using Probe A (Fig. 2A and 2B). DNA species of interest, DSBs and COs, were quantified using a phosphoimage analyzer. Parental DNA species were detected at 5.9 kb for maternal chromosomes and 4.3 kb for paternal chromosomes (Fig. 2A and 2B). DSB signals appeared at 3.0 kb and 3.3 kb in one-dimensional (1D) gel electrophoresis. Native/native two-dimensional (2D) gel electrophoresis was performed to detect joint molecules (JMs; SEI and dHJ; Fig. 2D and 2E). COs and NCOs were distinguished in 1D gels at 4.6 kb and 4.3 kb, respectively (Fig. 2A and 2F).

Repair of meiotic double-strand breaks progressed normally in *ku70Δ* cells

In WT cells, DSBs were initiated after 2.5 h and peaked at 4 h with approximately 16.7% hybridizing DNA species that then disappeared after 6 h. DSB levels and turnover were similar between WT and *ku70Δ* cells (Fig. 2B and 2C). Similar data for another set of physical analysis

UNCORRECTED PROOF

of independent time course experiments are presented in Supplemental Fig. 1. The maximum level of COs and NCOs in WT cells was 3.8% and 3.1%, respectively. The levels and turnover of COs and NCOs in *ku70Δ* cells were similar to those of WT cells, consistent with our meiotic division findings (Fig. 1 and Fig. 2G). To examine whether the Ku complex affects homolog bias, we performed 2D gel electrophoresis to observe JMs (Fig. 2E). Several types of JMs were detected using 2D gel analysis including intersister SEIs (IS-SEIs), IH-SEIs, IH-dHJs, and IS-dHJs. Consistent with our previous results for WT cells, IH-dHJ levels were higher than IS-dHJs at a ratio of 5:1 (Fig. 2E). Moreover, the ratio of IH-dHJs and IS-dHJs in *ku70Δ* cells was also 5:1. Additionally, IH-SEIs occurred at high levels in both WT and *ku70Δ* cells. Thus, the results indicate that the Ku complex is not required for the formation of JMs (DSB-to-JM transition) and establishment of homolog bias.

DSBs levels are reduced at the *HIS4LEU2*, *ARG4*, *BUD23*, and *CYS3* loci in *rad50S ku70Δ* cells

In *rad50S* mutant cells, the MRX complex is inactivated and thus DSBs accumulate instead of forming CO and NCO recombinants (30). Thus, the total number of DSBs can be measured from the *rad50S* allele, which is blocked at the DSB-to-JM transition. Surprisingly, the *rad50S* cells exhibited strong MMS sensitivity, but the *ku70Δ* mutation partially suppressed DNA damage of *rad50S* cells (Fig. 3A). Similar results were obtained when *rad50Δ* and *rad50Δ ku70Δ* cells were examined in the same experiments (Fig. 3B). These results indicate that damaged DNA is possibly repaired during NHEJ and DSB resection deficiency. To investigate whether the Ku complex is required for DSB formation, we used 1D gel electrophoresis for *rad50S* DSB analysis at the *HIS4LEU2*, *ARG4*, *BUD23*, and *CYS3* loci (Fig 3C and 3D). Notably, total levels of DSBs in *rad50S ku70Δ* cells were lower than those of WT cells at all

UNCORRECTED PROOF

loci. Furthermore, a significant subset of DSBs in *rad50S ku70Δ* cells were repaired to form COs at the *HIS4LEU2* hotspot, which can distinguish between IH-COs and IS-COs (Fig. 4A and 4B). Thus, a portion of DSBs in *rad50S ku70Δ* cells progressed to form COs at a later time point (from the middle of prophase during meiosis), indicating that cells repaired DSBs via the recombination pathway.

Ku70 is involved in DSB repair during arrest of the DSB end resection process

At the *HIS4LEU2* locus in *rad50S ku70Δ* cells, a subset of DSBs progressed to COs at a much later time point (Fig. 4A). This finding suggests that the COs detected in *rad50S ku70Δ* cells may result from meiotic recombination, implying that nucleolytic resection of DSB ends occurred in the absence of the Ku complex and a functional MRX complex. We further investigated the formation of COs and NCOs in *rad50S ku70Δ* mutant cells. Notably, COs and NCOs were detected in *rad50S ku70Δ* cells but not in *rad50S* cells (Fig. 4B and 4C). In *rad50S ku70Δ*, NCOs appeared after approximately 8 h and COs appeared after 10 h, indicating that NCOs formed earlier than COs. Interestingly, the maximum levels of COs were attained by 24 h. Therefore, our findings indicate that DSB repair occurred to form CO and NCO through meiotic recombination starting from the middle/late prophase phase in *rad50S ku70Δ* mutant cells.

DISCUSSION

DSBs can arise from diverse reactive metabolites, ionizing radiation, or stalling of DNA replication during cell cycle. Inappropriate repair of DSBs leads to cell death, senescence, or cancer. Two distinct DNA repair pathways, NHEJ and homologous recombination, eliminate DSBs depending on the cell cycle phase or the nature of DSB end process. During meiosis,

UNCORRECTED PROOF

cells induce programmed DSBs that are generated by Spo11 and accessory factors. The post-DSB role of Exo1 and the MRX complex is essential for promoting recombination. It has been reported that the MRX complex, in coordination with Sae2, mediates ssDNA nick formation and exhibits 3′ to 5′ exonuclease activity that resects the ssDNA towards Spo11-binding regions. Additionally, Exo1 and the Dna2-Sgs1 complex promote formation of long stretches of ssDNA that can be used for homology searching on homologous chromosomes during meiosis. The long single-stranded overhangs of DSBs are bound by the homology search and strand exchange proteins Rad51, Dmc1, and accessory factors including Rad52, Rad54, Rad54, Rad57, the PCSS complex, Hed1, Rdh54/Tid1, Hop-Mnd1, and Mei5-Sae3 (21). The MRX/N complex has been implicated in NHEJ-mediated DSB repair during mitosis in budding yeast. However, Ku complex-mediated NHEJ is dispensable in meiotic recombination of budding yeast (Fig. 4D), whereas it is essential for the successful maintenance of genomic integrity in mammalian cells (26, 27). The absence of NHEJ and a functional MRX complex in *Caenorhabditis elegans* channeled meiotic DSB repair to the exonuclease-dependent recombination pathway from NHEJ pathway (31). The absence of an MRX complex showed no meiotic DSB-to-JM transition or CO and NCO recombinants, as evidenced by physical analysis of recombination in budding yeast. The presence of unprocessed DSBs induces a checkpoint signal requiring pachytene checkpoint protein 2 (Pch2) that functions with Tel1 and the MRX complex (32). Thus, we theorized that the MRX complex possibly acts together with Pch2 to promote normal meiotic recombination. We can further suggest that absence of the MRX complex may induce the expression of NHEJ-related DNA repair proteins during meiosis. Herein, we observed diverse recombination phenotypes as follows, (i) meiotic recombination and nuclear division progressed normally in the absence of Ku70 as in WT cells; (ii) DSB levels were found reduced at various loci of yeast chromosomes in *rad50S ku70Δ* cells; (iii) a large portion of DSBs formed CO and NCO recombinants starting from the middle of prophase

UNCORRECTED PROOF

during meiosis; and (iv) a subset of DSBs remained unrepaired for 24 h. Our results indicate that some DSBs were repaired via NHEJ in meiotic cells that showed defective recombination due to the absence of the MRX complex. Moreover, in the absence of a functional NHEJ and MRX complex, recombination occurred starting from the middle of prophase, leading to CO and NCO formation. In WT cells, the Ku complex was not essential for CO and NCO formation, as the MRX complex and Exo1/Dna2-Sgs1 function in forming ssDNA overhangs of DSBs (33). When both the MRX complex and NHEJ were defective, Exo1/Dna2-Sgs1 may have functioned to expose ssDNA through their 5′ end resection activity, although this activity was not fully active without the initial strand nicking by the MRX complex (Fig. 4D).

In the present study, we found that the Ku complex is involved in meiotic DSB repair via NHEJ in the absence of MRX activity, but not the presence of the MRX complex. Our findings suggest that a portion of DSBs induced by Spo11 at early prophase or additional DSBs at late prophase may serve as NHEJ-mediated DSB repair sites during meiosis. These findings are important for understanding how cells deal with programmed DSBs (or endogenous damage-induced DSBs) during meiosis and how defective DSB end resection affects meiotic recombination in the presence or absence of another repair pathway.

MATERIALS AND METHODS

Yeast strains

We used the *Saccharomyces cerevisiae* SK1 strain in this study. Detailed information regarding strains is listed in Supplemental Materials Table. S1.

MMS sensitivity test

Cell were grown in YPD liquid medium (1% bacto yeast extract, 2% bacto peptone, and 2% glucose) for 24 h. Cells were diluted 10^{-1}, 10^{-2}, 10^{-3}, 10^{-4}, and 10^{-5} in distilled water and spotted

UNCORRECTED PROOF

ARTICLE IN PRESS

on YPD plates (1% bacto yeast extract, 2% bacto peptone, 2% bacto agar, and 2% glucose) and YPD plates containing 0.01% and 0.03% MMS. The plates were then incubated for 2 days.

Spore viability test

Diploid cells were grown in SPM (1% potassium acetate, 0.02% raffinose, and 0.01% antifoam) for 24 h. Spores were plated onto YPD plates through tetrad dissection and then incubated for 2 days.

Meiotic division

Cells in SPM were harvested at different time points, fixed in sorbitol solution (40% ethanol and 0.1 M sorbitol). Cells were then stained with DAPI (1 µl/mL) and the nuclei were counted (n = 200). Nuclei stained with DAPI were observed using fluorescence microscopy (Eclipse Ti-E; Nikon, Tokyo, Japan) and imaged using the Nikon DS-Qi2.

Meiotic time course analysis

Meiotic time course was performed as described previously (8-11). Cells were streaked onto YPG plates (1% bacto yeast extract, 2% bacto peptone, 2% bacto agar, and 3% glycerol) and incubated overnight. Cells were diluted onto YPD plates and incubated for 2 days. Single colonies were then incubated in YPD liquid media for 18 h. To synchronize cells in G1 phase, a 1/500 dilution of YPD culture was added to SPS (0.5% bacto yeast extract, 1% bacto peptone, 1% potassium acetate, 0.05 M potassium biphthalate, 0.5% ammonium sulfate, and 0.17% yeast nitrogen base without amino acids; pH 5.5) in a shaking incubator for 18 h. Synchronized cells were then transferred to SPM. Meiotic cells were harvested at different time points and crosslinked with psoralen (Sigma-Aldrich, St. Louis, MO) using ultraviolet light at 365 nm for 15 mins.

UNCORRECTED PROOF

ARTICLE IN PRESS

Physical analysis of meiotic recombination

Physical analysis was performed as described previously (8, 9). Detailed information regarding the procedures is described in Supplemental Materials.

ACKNOWLEDGMENTS

This work was supported by grants to K.P.K. from the National Research Foundation of Korea (NRF) funded by the Korean Ministry of Science, ICT and Future Planning (MSIT; NRF-2017R1A2B2005603; NRF-2018R1A5A1025077) and the Next-Generation BioGreen 21 Program (SSAC; No. PJ01322801), Rural Development Administration, Republic of Korea.

CONFLICTS OF INTEREST

There are no conflicts of interest.

FIGURE LEGENDS

Fig. 1. Ku70 is not essential for meiotic progression.

(A) Meiotic progression of WT and *ku70Δ* cells. Meiosis was induced in synchronized yeast in SPM and cell divisions were counted at the indicated time points. The error bar represents the standard deviation (SD; n = 3). (B) Representative images of DAPI-stained nuclei of WT and *ku70Δ* strains cultured in SPM for 24 h. Scale bar = 2.5 μm. (C) Analysis of spore viability in WT and *ku70Δ* strains (n > 100). (D) MMS sensitivity test. Cells were serially diluted and spotted onto YPD plates and YPD plates containing 0.01% and 0.03% MMS.

Fig. 2. Normal progression of meiotic DSB repair and formation of COs and NCOs in the absence of Ku70.

UNCORRECTED PROOF

(A) Physical map of the recombination assay for chromosome III. The *HIS4LEU2* hotspot schematic includes restriction enzyme polymorphisms and the Southern blot probe (probe A). (B) 1D gel electrophoresis of WT and *ku70Δ* strains. Cells were harvested at different time points (0, 2.5, 3.5, 4, 5, 6, 7, 8, 10, and 24 h). (C) Quantitative analysis of DSBs in WT and *ku70Δ* cells. (D) Structure of the 2D gel analysis of the *HIS4LEU2* locus. (E) 2D gel electrophoresis of WT cells. The average ratio of IH:IS-dHJ was 5:1 for both WT and *ku70Δ* cells. (F) Gel analysis of COs and NCOs. (G) Quantification of IH-COs and IH-NCOs in WT and *ku70Δ* cells. Error bars represent SD (n = 3) and significance was determined by a Student t test. Maternal species, paternal species, DSBs, double-strand breaks; IH-COs, interhomolog crossovers; IH-NCOs, interhomolog non-crossovers. SEI, single end invasion; IH-dHJs, interhomolog-double Holliday junction; IS-dHJs, intersister-double Holliday junction.

Fig. 3. The absence of Ku70 reduces DSB levels in a *rad50* background

(A) MMS sensitivity test of *rad50S* and *rad50S ku70Δ* cells. (B) MMS sensitivity test of *rad50Δ* and *rad50Δ ku70Δ* cells. (C) 1D gel electrophoresis of *rad50S* and *rad50S ku70Δ* of the *HIS4LEU2, ARG4, BUD23,* and *CYS3* loci. (D) Maximum level of DSBs at each hotspot locus. Error bars represent SD (n = 3).

Fig. 4. Absence of Ku70 and a functional MRX complex promotes CO and NCO formation

(A) Representative images of CO and NCO gels in *rad50S* and *rad50S ku70Δ*. (B) Quantitative analysis of COs and NCOs in *rad50S* and *rad50S ku70Δ* cells. Error bars represent SD (n = 3). (C) Maximum level of COs and NCOs in *rad50S* and *rad50S ku70Δ* cells. Error bars represent SD (n = 3) and significance was determined by a Student t test. **P < 0.01, ***P < 0.001. (D)

UNCORRECTED PROOF

Proposed model for the roles of the MRX complex and NHEJ pathway in meiotic recombination. DSBs are catalyzed by Spo11 and the MRX complex plays a role in DNA resection and Spo11-oligonucleotide release (34). Exo1 and the Dna2-STR complex promote additional DSB end resection to create long ssDNA overhangs. In the absence of NHEJ and a functional MRX complex, ~50% of DSBs progressed to recombination to form COs and NCOs (this study). STR, Sgs1-Top3-Rmi1; SDSA, synthesis-dependent strand annealing.

REFERENCES

1. Chung W-H (2014) To peep into Pif1 helicase: Multifaceted all the way from genome stability to repair-associated DNA synthesis. Journal of Microbiology 52, 89-98
2. Choi D-H, Lee R, Kwon S-H, Bae S-H (2013) Hrq1 functions independently of Sgs1 to preserve genome integrity in Saccharomyces cerevisiae. Journal of Microbiology 51, 105-112
3. Sung P (2018) Introduction to the Thematic Minireview Series: DNA double-strand break repair and pathway choice. Journal of Biological Chemistry 293, 10500-10501
4. Haber JE (2018) DNA Repair: The Search for Homology. BioEssays 40, 1700229
5. Fouquin A, Guirouilh-Barbat J, Lopez B, Hall J, Amor-Guéret M, Pennaneach V (2017) PARP2 controls double-strand break repair pathway choice by limiting 53BP1 accumulation at DNA damage sites and promoting end-resection. Nucleic Acids Research 45, 12325-12339
6. Daley JM, Laan RLV, Suresh A, Wilson TE (2005) DNA Joint Dependence of Pol X Family Polymerase Action in Nonhomologous End Joining. Journal of Biological Chemistry 280, 29030-29037
7. Cannavo E, Johnson D, Andres SN et al (2018) Regulatory control of DNA end

UNCORRECTED PROOF

resection by Sae2 phosphorylation. Nature Communications 9, 4016

8. Kim KP, Weiner BM, Zhang L, Jordan A, Dekker J, Kleckner N (2010) Sister cohesion and structural axis components mediate homolog bias of meiotic recombination. Cell 143, 924-937
9. Hong S, Sung Y, Yu M, Lee M, Kleckner N, Kim KP (2013) The logic and mechanism of homologous recombination partner choice. Mol Cell 51, 440-453
10. Hong S and Kim KP (2013) Shu1 promotes homolog bias of meiotic recombination in Saccharomyces cerevisiae. Mol Cells 36, 446-454
11. Yoon SW, Lee MS, Xaver M et al (2016) Meiotic prophase roles of Rec8 in crossover recombination and chromosome structure. Nucleic Acids Res 44, 9296-9314
12. Marcon E and Moens PB (2005) The evolution of meiosis: Recruitment and modification of somatic DNA-repair proteins. Bioessays 27, 795-808
13. Lam I and Keeney S (2015) Mechanism and regulation of meiotic recombination initiation. Cold Spring Harbor perspectives in biology 7, a016634-a016634
14. Gobbini E, Cassani C, Villa M, Bonetti D, Longhese MP (2016) Functions and regulation of the MRX complex at DNA double-strand breaks. Microbial Cell 3, 329-337
15. Seeber A, Hegnauer AM, Hustedt N et al (2016) RPA Mediates Recruitment of MRX to Forks and Double-Strand Breaks to Hold Sister Chromatids Together. Molecular Cell 64, 951-966
16. Chen H, Donnianni RA, Handa N et al (2015) Sae2 promotes DNA damage resistance by removing the Mre11–Rad50–Xrs2 complex from DNA and attenuating Rad53 signaling. Proceedings of the National Academy of Sciences of the United States of America 112, E1880-E1887
17. Hefferin ML and Tomkinson AE (2005) Mechanism of DNA double-strand break

UNCORRECTED PROOF

ARTICLE IN PRESS

repair by non-homologous end joining. DNA Repair 4, 639-648

18. Huertas P and Jackson SP (2009) Human CtIP Mediates Cell Cycle Control of DNA End Resection and Double Strand Break Repair. The Journal of Biological Chemistry 284, 9558-9565
19. Huertas P, Cortés-Ledesma F, Sartori AA, Aguilera A, Jackson SP (2008) CDK targets Sae2 to control DNA-end resection and homologous recombination. Nature 455, 689-692
20. Mimitou EP and Symington LS (2011) DNA end resection - unraveling the tail. DNA repair 10, 344-348
21. Kim KP and Mirkin EV (2018) So similar yet so different: The two ends of a double strand break. Mutation Research/Fundamental and Molecular Mechanisms of Mutagenesis 809, 70-80
22. Tsukamoto Y, Kato J, Ikeda H (1996) Hdf1, a yeast Ku-protein homologue, is involved in illegitimate recombination, but not in homologous recombination. Nucleic Acids Research 24, 2067-2072
23. Gu Y, Jin S, Gao Y, Weaver DT, Alt FW (1997) Ku70-deficient embryonic stem cells have increased ionizing radiosensitivity, defective DNA end-binding activity, and inability to support V(D)J recombination. Proceedings of the National Academy of Sciences of the United States of America 94, 8076-8081
24. Sorenson KS, Mahaney BL, Lees-Miller SP, Cobb JA (2017) The non-homologous end-joining factor Nej1 inhibits resection mediated by Dna2–Sgs1 nuclease-helicase at DNA double strand breaks. The Journal of Biological Chemistry 292, 14576-14586
25. Pannunzio NR, Watanabe G, Lieber MR (2018) Nonhomologous DNA end-joining for repair of DNA double-strand breaks. Journal of Biological Chemistry 293, 10512-10523

UNCORRECTED PROOF

26. Lieber MR (2010) The mechanism of double-strand DNA break repair by the nonhomologous DNA end-joining pathway. Annual review of biochemistry 79, 181-211
27. Lieber MR (2008) The Mechanism of Human Nonhomologous DNA End Joining. Journal of Biological Chemistry 283, 1-5
28. Lee MS, Yoon SW, Kim KP (2015) Mitotic cohesin subunit Mcd1 regulates the progression of meiotic recombination in budding yeast. J Microbiol Biotechnol 25, 598-605
29. Cho HR, Kong YJ, Hong SG, Kim KP (2016) Hop2 and Sae3 Are Required for Dmc1-Mediated Double-Strand Break Repair via Homolog Bias during Meiosis. Mol Cells 39, 550-556
30. Hong S, Choi EH, Kim KP (2015) Ycs4 is Required for Efficient Double-Strand Break Formation and Homologous Recombination During Meiosis. J Microbiol Biotechnol 25, 1026-1035
31. Yin Y and Smolikove S (2013) Impaired Resection of Meiotic Double-Strand Breaks Channels Repair to Nonhomologous End Joining in Caenorhabditis elegans. Molecular and Cellular Biology 33, 2732-2747
32. Ho H-C and Burgess SM (2011) Pch2 Acts through Xrs2 and Tel1/ATM to Modulate Interhomolog Bias and Checkpoint Function during Meiosis. PLOS Genetics 7, e1002351
33. Hunter, N (2006) Meiotic Recombination. Molecular Genetics of Recombination, Topics in Current Genetics, Springer-Verlag, Heidelberg, 381-442
34. Neale M, Pan J and Keeney S (2005) Endonucleolytic processing of covalent protein-linked DNA double-strand breaks, nature 436, 1053-1057

UNCORRECTED PROOF

Figure 1

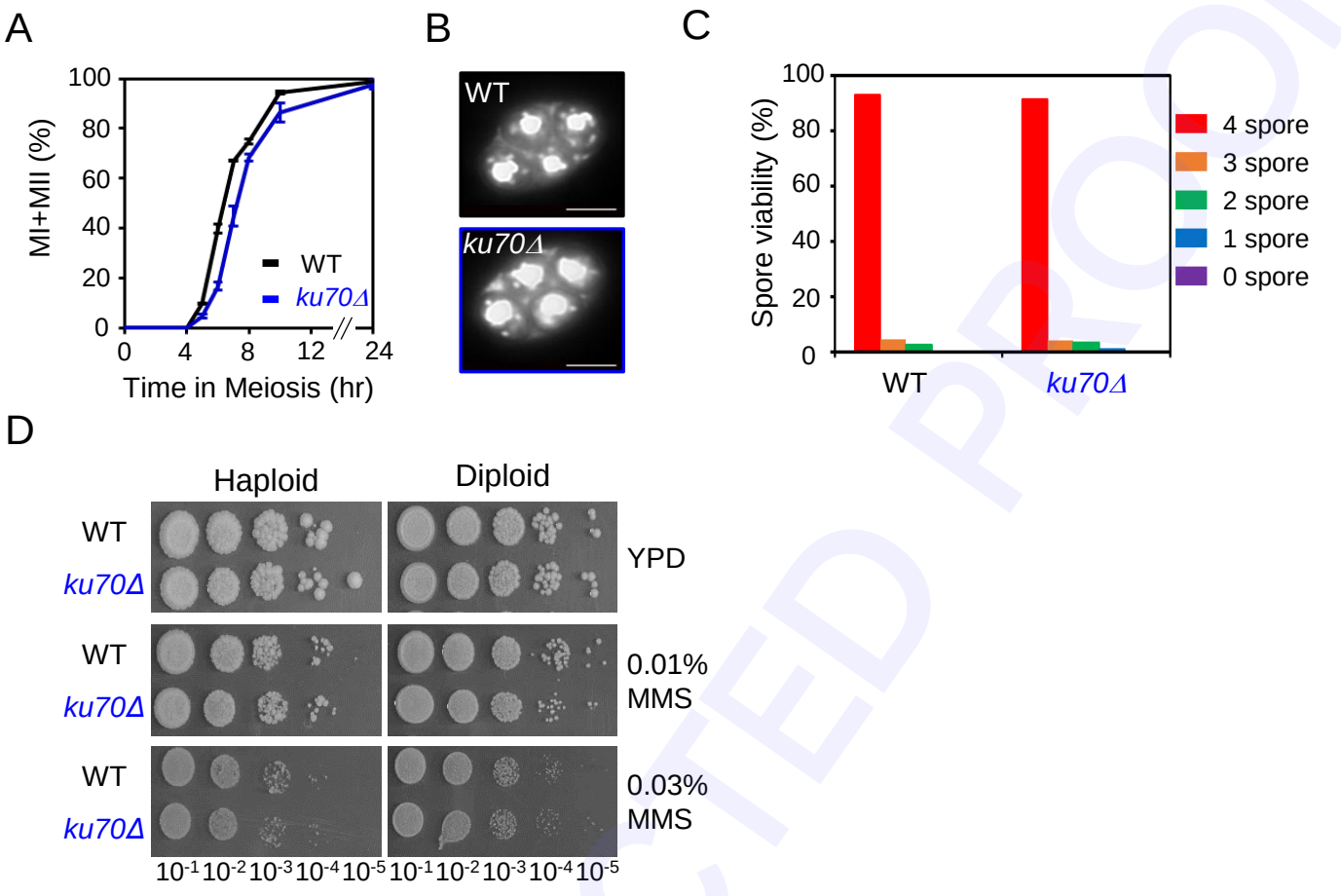

UNCORRECTED PROOF

Figure 2

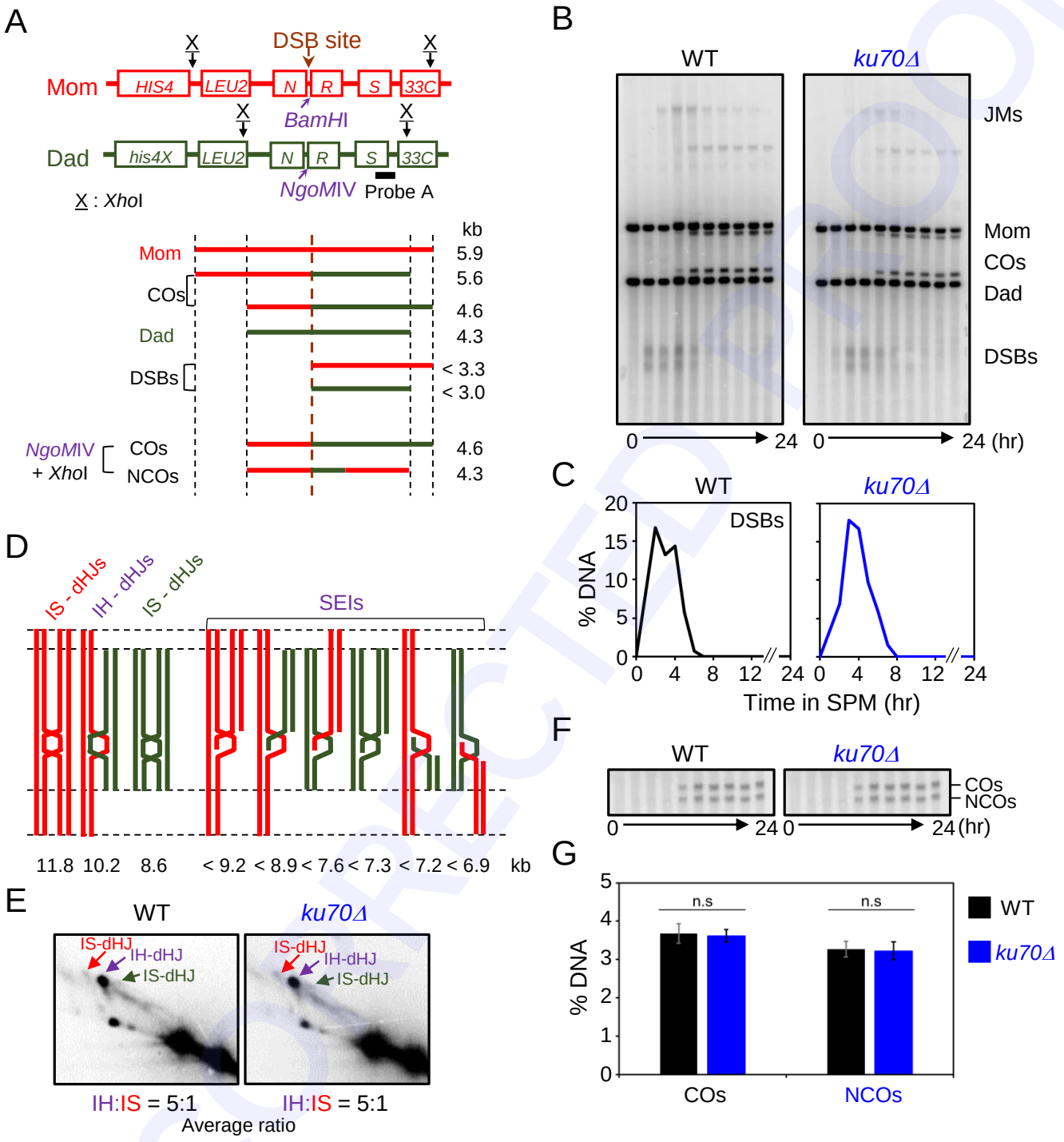

UNCORRECTED PROOF

Figure 3

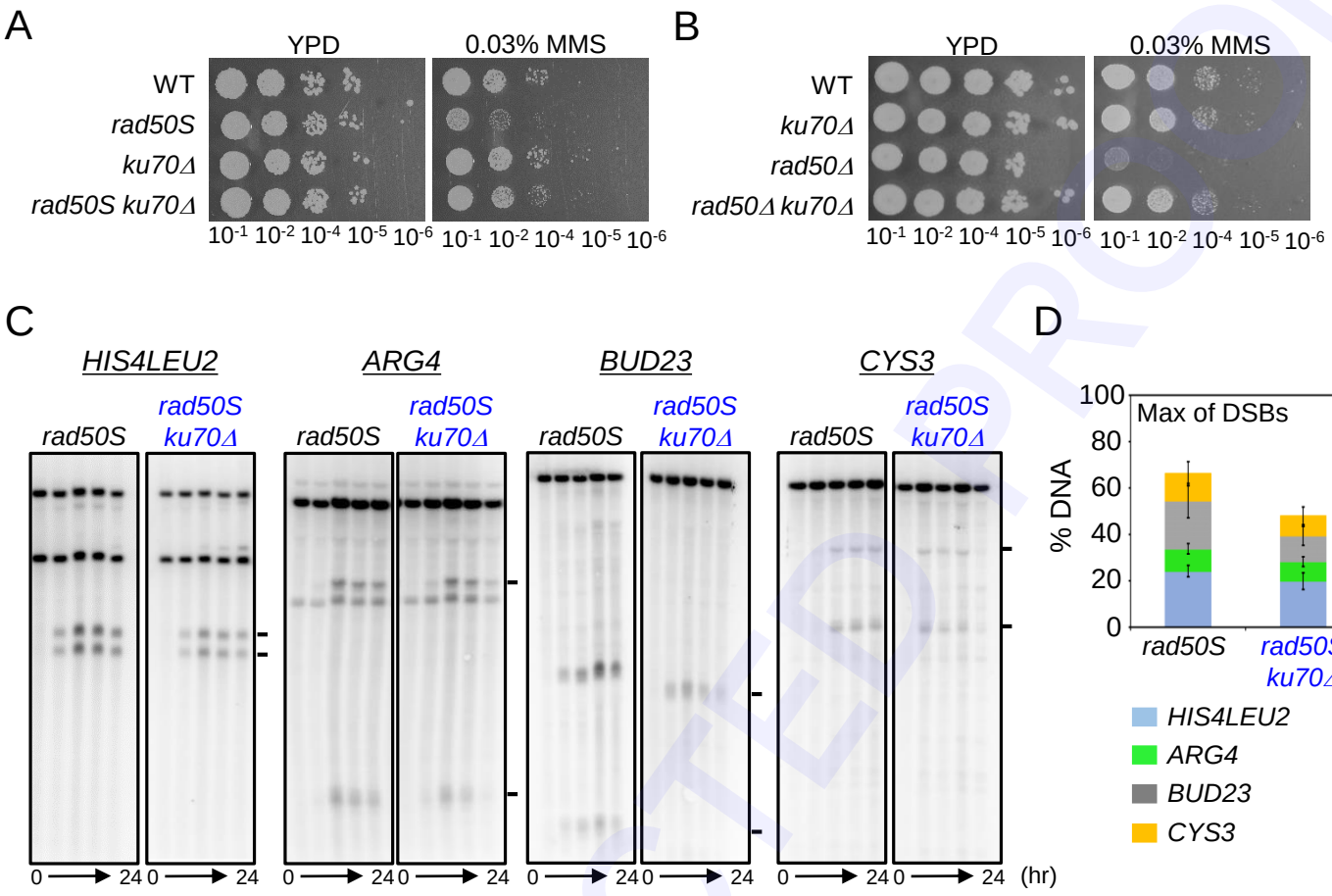

UNCORRECTED PROOF

Figure 4

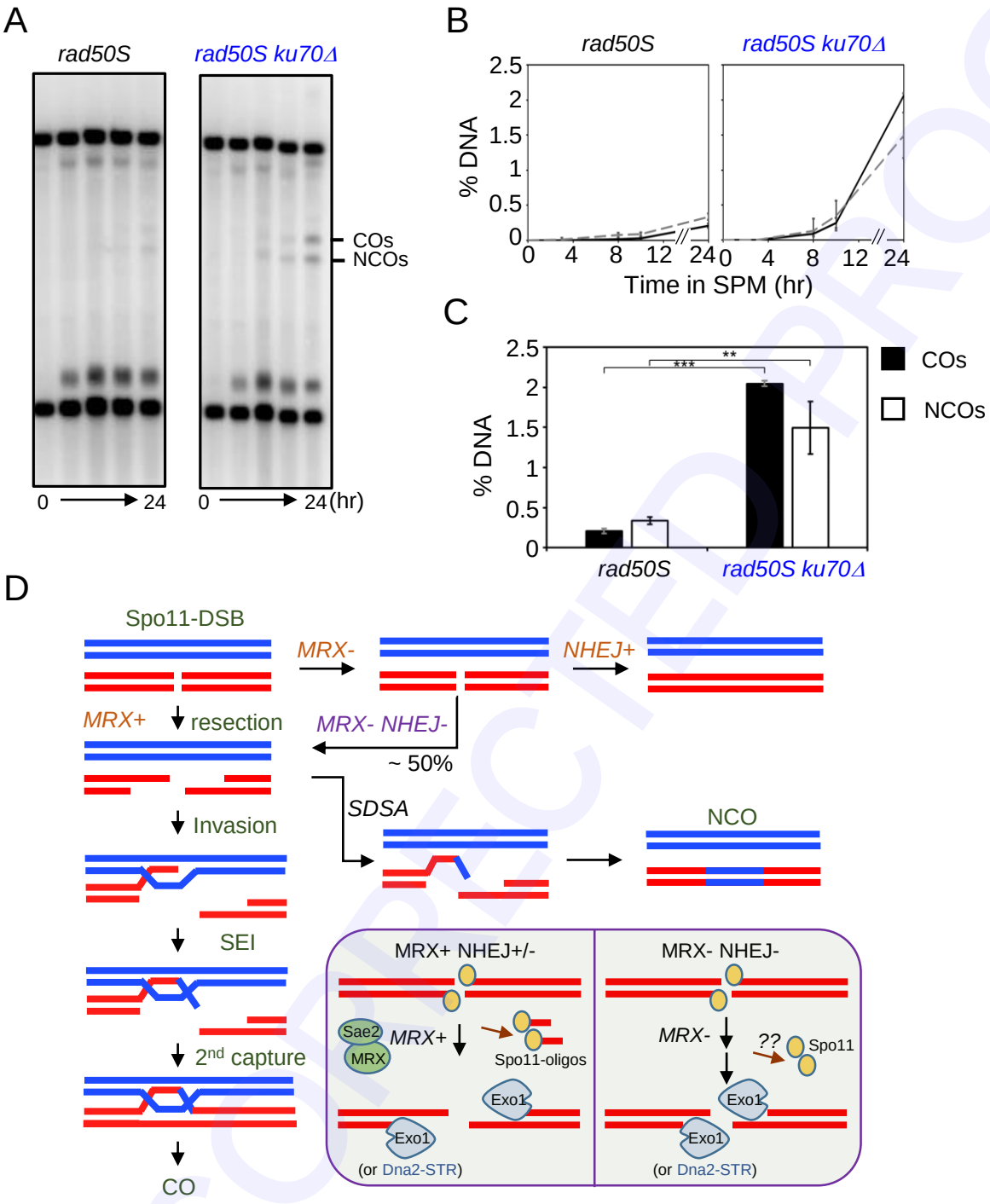

UNCORRECTED PROOF

ARTICLE IN PRESS

SUPPLEMENTARY MATERIALS

Supplemental Figure

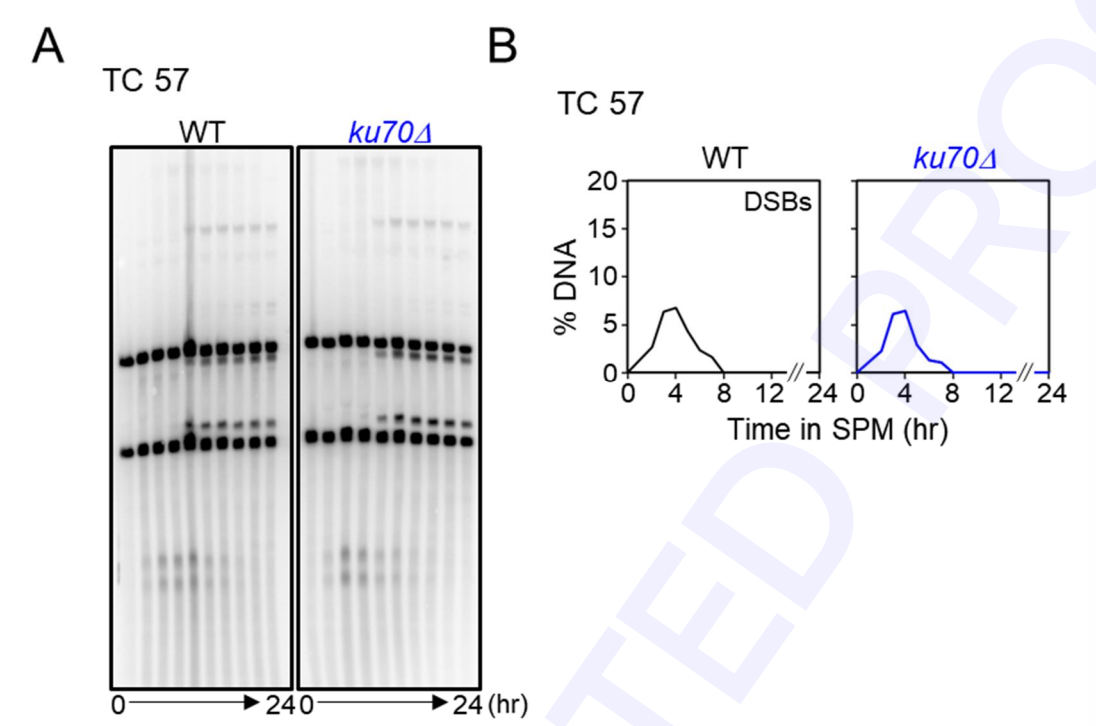

Figure S1. DSB analysis in WT and *ku70Δ* cells

(A) 1D gel electrophoresis of WT and *ku70Δ* cells. (B) Quantification of DSB levels in WT and *ku70Δ* cells.

UNCORRECTED PROOF

ARTICLE IN PRESS

Supplemental Materials and Methods

Physical analysis of meiotic recombination

For 1D gel analysis, 2 μg of DNA was digested with the XhoI restriction enzyme (Enzynomics, Daejeon, Korea) for 3 h at 37 ℃. DNA samples were loaded onto 0.6% SeaKem LE agarose gel (Lonza, Basel, Switzerland) in TBE buffer (89 mM Tris-borate and 2 mM EDTA; pH 8.3) and run at ~2 V/cm for 24 h. For 2D gel analysis, 2.5 μg of DNA was digested with XhoI for 3 h at 37 ℃, after which the samples were loaded onto 0.4% SeaKem Gold agarose gel in TBE buffer and run at 1 V/cm for 21 h. Gels were stained with 0.5 μg/mL ethidium bromide for 30 min and then gel strips were cut and placed on a 2D gel tray. 2D gel electrophoresis was performed using 0.8% SeaKem LE agarose gel in TBE buffer at ~6 V/cm for 6 h at 4 ℃. For CO and NCO gel analysis, 2 μg of DNA was digested with XhoI and NgoMIV for 6 h at 37 ℃. DNA samples were then loaded onto 0.6% SeaKem LE agarose gel in TBE buffer and run at ~2 V/cm for 24 h. Gels were subjected to Southern blot analysis after transferring the DNA species onto a nylon-membrane (Pall Corporation, New York, NY). Hybridization was carried out using probe A labeled with ^{32}P-dCTP radioactive nucleotides in a random primer labeling kit mixture (Agilent Technologies, Santa Clara, CA). Quantification of DNA species was performed using a phosphoimage analyzer and DNA signals were quantified by the Quantity One software (Bio-Rad Laboratories, Hercules, CA).

Table S1. *S. cerevisiae* strains used in this study.

UNCORRECTED PROOF

ARTICLE IN PRESS

Strain†	Genotype
KKY4278	*MATa/MATα HIS4::LEU2-(BamHI)/his4x::LEU2-(NgoMIV)--URA3,*
KKY4	*MATα HIS4::LEU2-(BamHI), nuc1Δ::hygroB*
KKY476	*MATa/MATα HIS4::LEU2-(BamHI)/his4x::LEU2-(NgoMIV)--URA3, nuc1Δ::hygroB, ku70Δ::KanMX4*
KKY453	*MATa HIS4::LEU2-(BamHI), nuc1Δ::hygroB, ku70Δ::KanMX4*
KKY885	*MATa/MATα HIS4::LEU2-(BamHI)/his4x::LEU2-(NgoMIV)--URA3, nuc1Δ::hygroB, rad50S::URA3*
KKY1141	*MATa/MATα HIS4::LEU2-(BamHI)/his4x::LEU2-(NgoMIV)--URA3, nuc1Δ::hygroB, ku70Δ ::KanMX4, rad50S::URA3*
KKY4755	*MATa/MATα HIS4::LEU2-(BamHI)/his4x::LEU2-(NgoMIV)--URA3, rad50Δ::KanMX4, ku70Δ:: KanMX4,*
KKY4771	*MATa/MATα HIS4::LEU2-(BamHI)/his4x::LEU2-(NgoMIV)--URA3, rad50Δ::KanMX4*

41

UNCORRECTED PROOF